A Chemical Strategy for Intracellular Arming of an Endogenous Broad-Spectrum Antiviral Nucleotide

Kellan T. Passow, Haley S. Caldwell, Kiet A. Ngo, Jamie J. Arnold, Nicole M. Antczak, Anoop Narayanan, Joyce Jose, Shana J. Sturla, Craig E. Cameron, Alexander T. Ciota, and Daniel A. Harki*

ABSTRACT: The naturally occurring nucleotide 3′-deoxy-3′,4′-didehydro-cytidine-5′-triphosphate (**ddhCTP**) was recently found to exert potent and broad-spectrum antiviral activity. However, nucleoside 5′-triphosphates in general are not cell-permeable, which precludes the direct use of **ddhCTP** as a therapeutic. To harness the therapeutic potential of this endogenous antiviral nucleotide, we synthesized phosphoramidate prodrug HLB-0532247 (**1**) and found it to result in dramatically elevated levels of **ddhCTP** in cells. We compared **1** and 3′-deoxy-3′,4′-didehydro-cytidine (**ddhC**) and found that **1** more effectively reduces titers of Zika and West Nile viruses in cell culture with minimal nonspecific toxicity to host cells. We conclude that **1** is a promising antiviral agent based on a novel strategy of facilitating elevated levels of the endogenous **ddhCTP** antiviral nucleotide.

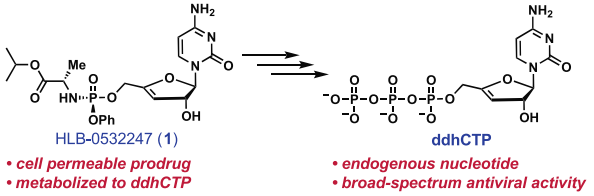

INTRODUCTION

Nucleoside analogs targeting viral polymerases are critically important therapeutics with proven efficacy against a spectrum of viruses.[1] Emerging viral threats such as SARS-CoV-2, West Nile (WNV), and Zika (ZIKV) are reminders that new therapeutics are needed. 3′-Deoxy-3′,4′-didehydro-cytidine-5′-triphosphate (**ddhCTP**, Figure 1) is a recently discovered endogenous antiviral nucleotide.[2] **ddhCTP** inhibits the polymerases of dengue (DENV), WNV, ZIKV, hepatitis C (HCV), and polio (PV, weak inhibition in competition with ribonucleoside 5′-triphosphates)[2] as well as SARS-CoV-2[3] via chain termination due to the lack of a 3′-alcohol. However, cellular studies with 3′-deoxy-3′,4′-didehydro-cytidine (**ddhC**, Figure 1) revealed only weak ZIKV inhibitory activity.[2] Harnessing the antiviral activity of **ddhCTP** through the use of a cell-permeable nucleoside 5′-monophosphate prodrug that can be metabolically activated to **ddhCTP** may confer a new broad-spectrum antiviral agent.

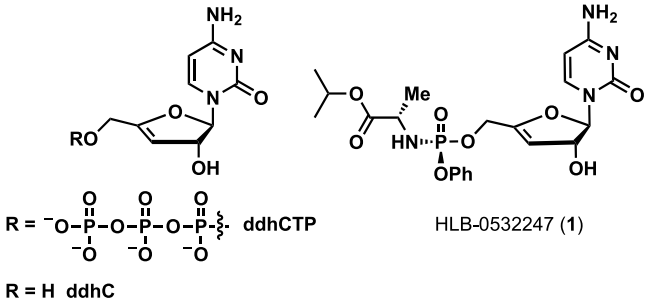

Figure 1. ddhCTP, **ddhC**, and HLB-0532247 (**1**).

Phosphoramidate prodrugs of nucleotides, including the ProTide class of modifications,[4−7] bypass the often rate-limiting 5′-monophosphorylation that occurs during the metabolism of nucleoside drugs into their bioactive 5′-triphosphates.[8−10] By bypassing this process, ProTides increase the efficacy of antiviral nucleosides[11−15] and has resulted in the discoveries of sofosbuvir[10] and tenofovir alafenamide.[16,17] To arm the cell with its endogenous antiviral defense molecule **ddhCTP**, we designed and synthesized HLB-0532247 (**1**), which is **ddhC** bearing the 5′-phosphoramidate moiety found in the hepatitis C drug sofosbuvir (Figure 1).[10] We show that **1** potently inhibits WNV and ZIKV in cell culture through intracellular production of **ddhCTP** to levels that surpass what cells or exogenous **ddhC** dosing can produce. Moreover, we show that **1** is nontoxic to host cells and is not used as a substrate by mitochondrial DNA polymerase γ, which is a known off-target of antiviral nucleosides/nucleotides.[18−21]

RESULTS AND DISCUSSION

The synthesis of HLB-0532247 (**1**) was completed using established methods for the preparation of nucleosides containing dehydrated ribose rings.[22−25] The synthesis of **1**

Received: August 20, 2021
Published: October 18, 2021

Scheme 1. Synthesis of HLB-0532247 (1) from Cytidine

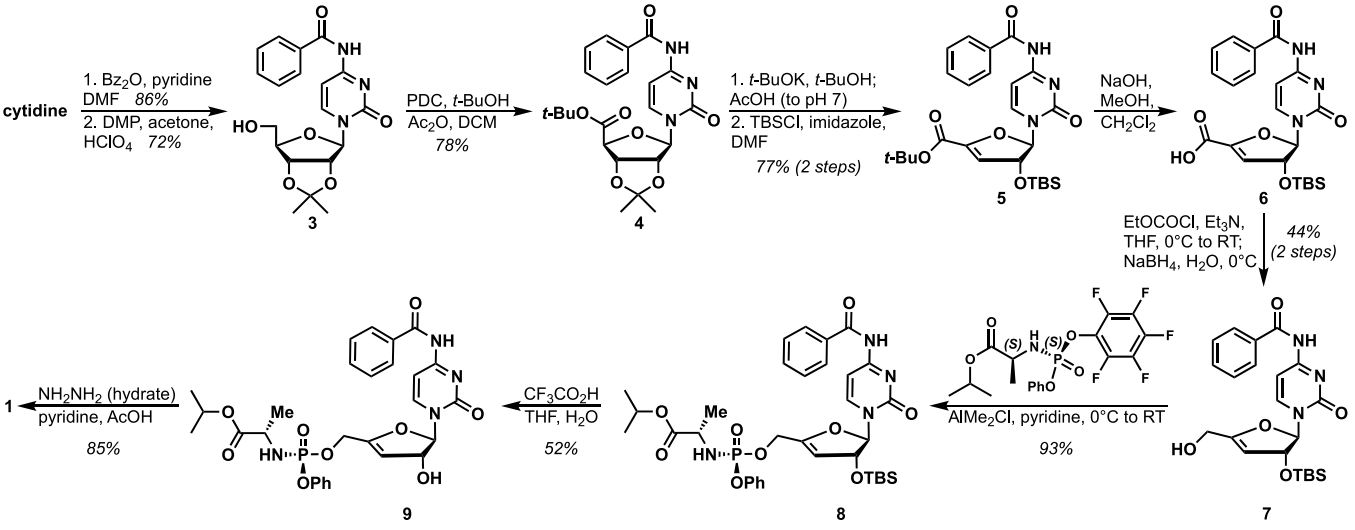

commences with a two-step protection sequence to yield bis-protected cytidine **3**,[26,27] which can undergo an oxidative esterification, affording **4** in 78% yield (Scheme 1).[28,29] Base-mediated tandem elimination and deprotection of **4** followed by reprotection of the 2′-alcohol with TBSCl gives **5** in 77% yield in a one-pot procedure.[22,23] Reduction of the carboxylic ester to the primary alcohol yields **7**. Nucleoside **7** was then converted to phosphoramidate **8** in 93% yield as a single *P*-diastereomer, which was assigned as *S* based on analogy to literature precedent in which in-line displacement of the pentafluorophenol by allylic alcohol **7** inverts the phosphorous stereochemistry yet retains the *S* configuration due to a change in priority.[30] Deprotection of the silyl group required acidic conditions to yield **9**, as the use of traditional fluoride deprotection strategies led to removal of the phosphoramidate, yielding the undesired product N4-benzoyl-**ddhC**. N4-benzoyl amide **9** was deprotected using buffered hydrazine[31] to produce **1** in high yield. **ddhC** was synthesized as previously described.[32]

The activity of **1** against virus-infected cells was investigated to determine whether the phosphoramidate prodrug offered significant potency improvements over **ddhC**. It has been shown previously that ZIKV levels in infected Vero cells were reduced by 50−200× upon exposure to 1 mM **ddhC** over 24 h.[2] To evaluate **1** similarly, Vero, HUH7, and HUH7.5 cell lines were treated with **1** and then infected with ZIKV (strain PRABC59) at a multiplicity of infection (MOI) of 0.1. Virus levels were quantified by plaque titration 4 days post-infection. **1** proved to be significantly more potent than **ddhC** against ZIKV, resulting in >1 $\log_{10}$ pfu/mL reduction in virus levels at 0.1 mM doses in both HUH7 and HUH7.5 cell lines, with weaker activity observed in Vero cells (Figure 2A). To directly compare the antiviral activity of **1** to **ddhC** against a different virus, Vero, HUH7, and HUH7.5 cells were treated with **1** or **ddhC** and then infected with WNV at an MOI of 0.1. At 3 days post-infection, we found **ddhC** to be ineffective against WNV across this panel of cell lines, in stark contrast to its published efficacy against ZIKV.[2] Excitingly, **1** reduced WNV levels in HUH7 and HUH7.5 cells by >4 $\log_{10}$ pfu/mL at 1.0 mM, but was inactive in Vero cells. These data demonstrate that introduction of the phosphoramidate moiety significantly promotes antiviral effects. Of additional note, we synthesized **1** as a mixture of *R* and *S* phosphorous diastereomers and observed no difference in

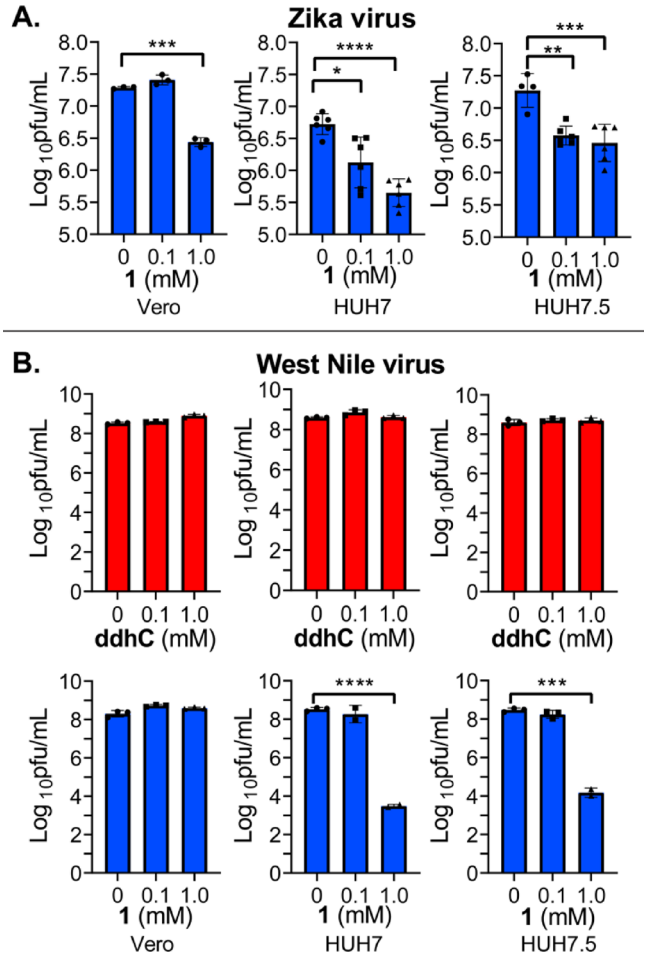

Figure 2. (A) Effect of **1** on ZIKV virus titer in a panel of cell lines. (B) Effect of **1** and **ddhC** on WNV virus titer in a panel of cell lines. **ddhC** results shown in red; **1** results shown in blue. The cell line tested is indicated in each column. *p < 0.05, **p < 0.01, ***p < 0.001, and ****p < 0.0001 (see Experimental Section for additional details).

antiviral activity in comparison to **1** (single diastereomer) in preliminary studies (data not shown).

We next evaluated whether **1** or **ddhC** is cytotoxic, which could obfuscate the observed antiviral activity. Many clinically

approved viral polymerase and reverse transcriptase inhibitors are toxic with chronic dosing due to off-target effects, often the result of human polymerase inhibition.[20,21] We found that neither **ddhC** nor **1** were cytotoxic to Vero or HUH7 cells after 2 days in culture (Figure S1). Extended assays to 5 days in culture revealed only modest toxicity (>60% cell viability at a 1.0 mM dose of **1**; Figure S1). In addition, we found that **ddhCTP** is not a substrate for DNA polymerase γ (Figure 3A), which is the

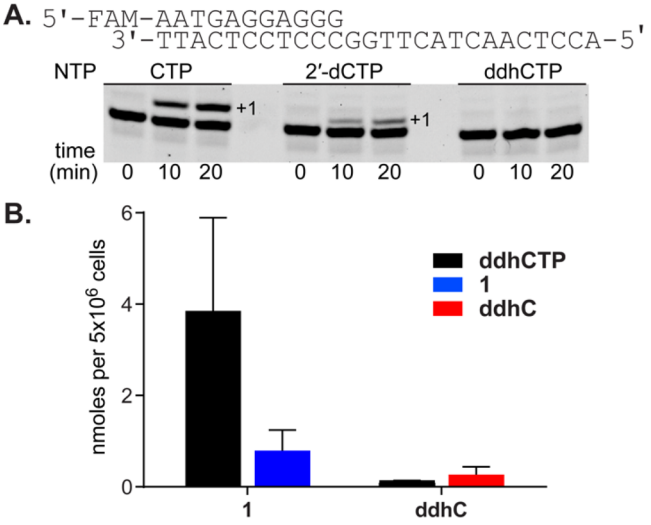

Figure 3. DNA polymerase γ (catalytic domain) was allowed to react with a FAM-labeled DNA primer (A) and a cytidine triphosphate analog (CTP, 2′-dCTP, and **ddhCTP**). Reactions were conducted for 0, 10, or 20 min. The presence of starting DNA (lower band) and addition products (n + 1 nt) was determined by gel electrophoresis analysis. (B) Metabolism of **1** and **ddhC** to **ddhCTP** in cells. Levels of analytes (**ddhCTP**, black; **1**, blue; **ddhC**, red) following treatment of HUH7 cells with **1** or **ddhC**. Background **ddhCTP** levels were <0.01 nmol per 5×10^6 HUH7 cells or below the limit of quantitation in each DMSO-only treatment replicate (data not shown). Values are mean ± SD (n = 3).

enzyme often associated with chronic toxicity due to the incorporation of nucleotide analogs into mitochondrial DNA.[18−21] These results suggest that **1** is devoid of common toxicity liabilities known for this class of compounds. The 50% cytotoxic concentration (CC_{50}) of **1** is greater than 1 mM, surpassing that of many other potent antiviral agents, including sofosbuvir and ribavirin, giving it an advantage in future development efforts.[33−36]

Prodrug **1** was next subjected to stability assays to gauge its suitability for systemic use and cell permeability assays (Figure S2). In the presence of human plasma, **1** was stable up to 2 h (>87% remaining). In simulated gastric fluid (SGF), approximately 76% of **1** remained after 6 h (Figure S2B). Taken together, these stability properties of **1** are suitable for future in vivo studies. Caco-2 permeability studies were also conducted, revealing that **1** has similar cell permeability properties to that reported for sofosbuvir in a related PAMPA assay (mean P_{app} of 0.3 nm/s for **1** compared to 0.46 nm/s for sofosbuvir; Figure S2C).[10]

We next investigated the conversion of **1** to **ddhCTP** in cells. Since we utilized the same phosphoramidate moiety (ProTide) in **1** as that found in sofosbuvir, we hypothesized that **1** likely utilizes the same enzymes for metabolic activation as sofosbuvir. Consequently, we first established that HUH7 cells express the phosphoramidase enzyme HINT1 (histidine triad nucleotide-binding protein 1), which is responsible for cleaving P−N bonds found in phosphoramidate prodrugs such as sofosbuvir.[11,37] Vero cells also express HINT1 but at lower levels (Figure S3). Carboxyesterase 1 (CES1) also is implicated in the metabolism of sofosbuvir,[11] and its expression levels in HUH7 cells are known to be high.[38] These data may suggest why **1** is more active in HUH7 versus Vero cells as also observed for sofosbuvir.[34] Second, we measured **ddhCTP** production in cells. DMSO, **ddhC**, and **1** were dosed to HUH7 cells at 100 μM for 24 h, and then the cell lysates were evaluated by mass spectrometry. In DMSO control-treated cells, basal levels of **ddhCTP** were found (<0.01 nmol per 5×10^6 cells or below the limit of quantitation). Both **1** and **ddhC** were detected in HUH7 lysate 24 h following dosage, indicating that both compounds are cell-permeable (Figure 3B). However, the amounts of the **ddhCTP** metabolite detected in the treated cells were vastly different: HUH7 cells treated with **1** produced 3.8 nmol of **ddhCTP** per 5 million cells, whereas cells treated with **ddhC** produced 0.13 nmol of **ddhCTP** per 5 million cells. Consequently, exposing cells to phosphoramidate **1** results in a 29-fold increase in **ddhCTP** compared with treatment of **ddhC**. If the HUH7 cell volume is approximated, the intracellular concentration of **ddhCTP** produced by exposure to **1** is greater than 1 mM (see Experimental Section for details).[39] This concentration far surpasses those arising from other methods of **ddhCTP** production, namely, HEK293 cells exposed to **ddhC** produced ~100 μM **ddhCTP** after 48 h, and macrophages (RAW 264.7) induced with IFNα produced 350 μM **ddhCTP** after 19 h.[2] Our results with **1** are similar to the concentrations of sofosbuvir triphosphate found in animal models and cell studies.[10,34] These data support the hypothesis that **1** undergoes a sequence of metabolic activations to the 5′-triphosphate in a manner analogous to sofosbuvir[11] and that **ddhCTP** is the source of the observed antiviral activity of **1**.

ddhCTP has been shown to inhibit a variety of viral polymerases including those of DENV, WNV, ZIKV, HCV, and SARS-CoV-2.[2,3] **ddhCTP** inhibits the polymerases by chain termination, preventing the synthesis of viral RNA beyond its own incorporation. To further study these processes, we report a chemical synthesis of **ddhCTP** that is free of contaminating CTP, which is a limitation of enzymatic preparations (Scheme S1).[2] Of note, another method for synthesizing **ddhCTP** was reported recently.[40] Using synthetic **ddhCTP** (Scheme S1) and ZIKV RdRp in a reported primer extension assay (Figure 4A and Figure S4),[41] we confirm that **ddhCTP** functions as expected for an obligate chain terminator. Building on these results, we show that **ddhCTP** potently inhibits ZIKV RdRp in a competitive fashion against 10 μM CTP (Figure 4). Enzymatic processing of **ddhCTP** inhibited production of full-length RNA in a dose-dependent manner (IC_{50} = 320 ± 10 μM) (Figure 4B,C).

CONCLUSIONS

In conclusion, we report the development of HLB-0532247 (**1**), which facilitates dramatically enhanced levels of **ddhCTP** in cells, yielding potent antiviral effects. Prodrug **1** is non-toxic to host cells and primer extension assays with mitochondrial DNA polymerase γ, an off-target for nucleotide-based drugs, show that **ddhCTP** is not a substrate. Taken together, **1** is a promising antiviral agent that merits further development. Moreover, our strategy of using **ddhC** prodrugs that are metabolically activated to **ddhCTP** offers opportunities to tailor physiochemical and

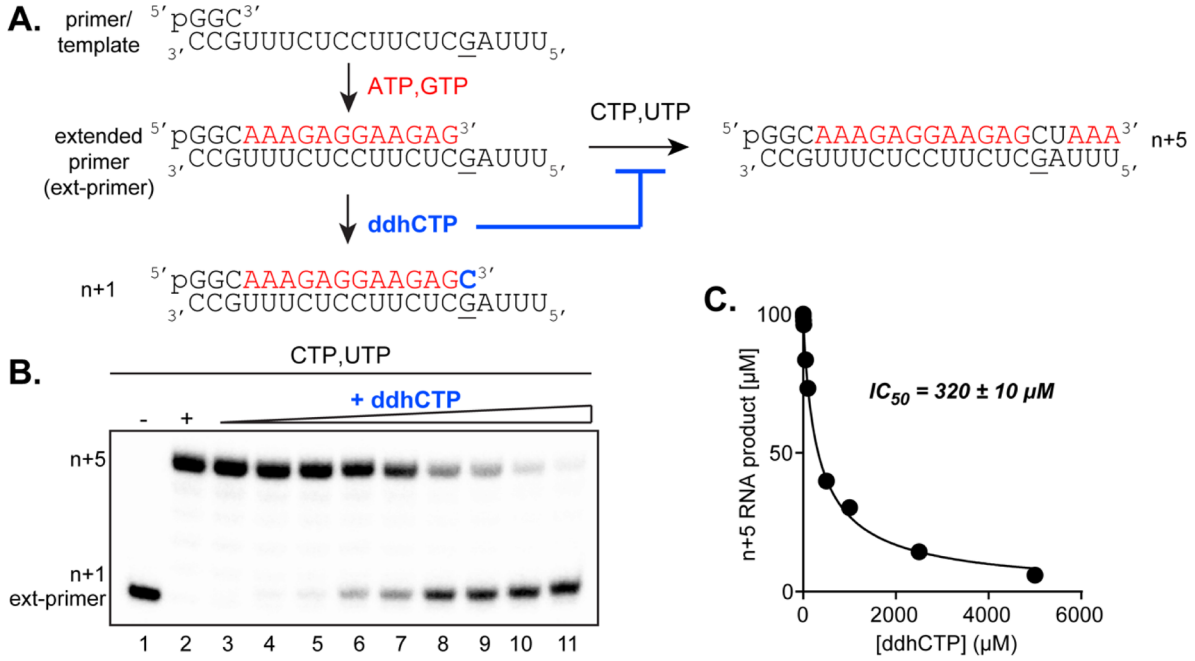

Figure 4. Synthetic **ddhCTP** is utilized as a substrate by ZIKV NS5 RdRp and chain-terminates RNA synthesis. (A) Schematic of the primer extension assay for evaluating chain-terminating activity in the presence of CTP. **ddhCTP** effectively competes for incorporation with CTP, resulting in the accumulation of the chain-terminated $n + 1$ product. (B) ZIKV RdRp-catalyzed nucleotide incorporation with increasing concentrations of **ddhCTP** (0, 1, 5, 10, 50, 100, 500, 1000, 2500, and 5000 μM) in the presence of 10 μM CTP. Lane 1 has no CTP or UTP. Lane 2 has CTP and UTP. Lanes 3−11 have CTP, UTP, and increasing amounts of competitor **ddhCTP**. (C) Representative plot of the percentage inhibition as a function of **ddhCTP** concentration and mean IC_{50} (with a standard error) from the individual curve fit data. All experiments were repeated independently 3× with similar results.

metabolic activation properties for various therapeutic applications.

EXPERIMENTAL SECTION

General Procedure. Reactions were performed in flame-dried glassware under inert gas (N_2 or Ar) and stirred using a Teflon-coated magnetic stir bar. Reaction solvents tetrahydrofuran (THF) and dichloromethane (DCM) were dried by passage over a column of activated alumina and dimethylformamide (DMF) over crushed molecular sieves using a solvent purification system (MBraun). Other solvents were purchased as ACS grade or higher and used as received unless otherwise noted. TMSCl was purified by short-path distillation.[42] Silica gel chromatography was accomplished using a Teledyne-Isco Combiflash Rf-200 instrument using Redisep Rf High Performance silica gel columns from Teledyne-Isco. ^{1}H NMR (500 MHz), ^{13}C NMR (125 MHz), and ^{31}P NMR (202 MHz) were collected on a Bruker Advance NMR spectrometer at room temperature. NMR chemical shifts (δ) were recorded relative to solvent signal for ^{1}H NMR (δ = 7.26 for $CDCl_3$, δ = 4.79 for D_2O, δ = 3.31 for MeOD, and δ = 2.50 for $(CD_3)_2SO$) and the solvent signal for ^{13}C NMR (δ = 77.0 for $CDCl_3$, δ = 49.0 for MeOD, and δ = 39.7 for $(CD_3)_2SO$). The high-resolution mass spectra were obtained at the Analytical Biochemistry Core Facility at the University of Minnesota Masonic Cancer Center using an LTP Orbitrap Velos mass spectrometer (Thermo Fisher). Compound purities of synthesized molecules were determined by analytical HPLC analysis using an Agilent 1200 series instrument with a diode array detector monitoring 215 or 254 nm. A Zorbax SB-C18 column (4.6 mm × 150 mm × 5.0 μm, Agilent Technologies) was used. A two-solvent system was used as the eluents: solvent A, distilled and deionized H_2O (containing 0.1% TFA); solvent B, MeCN (containing 0.1% TFA). The gradient (1 mL/min flow rate) consisted of the following: 90:10 A:B from 0 to 2 min, followed by a linear gradient to 20:80 A:B from 2 to 24 min, a second gradient to 5:95 A:B from 24 to 26 min, and an isocratic 5:95 A:B from 26 to 30 min. The purity of **ddhCTP** was determined by analytical HPLC analysis using an Agilent 1200 series instrument with a diode array detector monitoring 215 or 260 nm. A Zorbax SB-C18 column (4.6 mm × 150 mm × 5.0 μm, Agilent Technologies) was used. A two-solvent system was used as the eluents: solvent A, 100 mM aqueous KH_2PO_4 (pH 6); solvent B, MeCN. The gradient (1.0 mL/min flow rate) consisted of the following: 99:1 A:B from 0 to 5 min, followed by a linear gradient to 20:80 from 5 to 20 min.

Nucleosides and nucleoside prodrugs tested in biological assays were >95% (254 nm) and >90% (215 nm) pure by HPLC. Prodrug **1** (three batches) was 95−99% (254 nm) and 96−98% (215 nm) pure, **ddhC**[32] (three batches) was 95−99% (254 nm) and 90−99% (215 nm) pure, and synthesized **ddhCTP** was >99% (270 nm) and 94% (215 nm) pure by HPLC (see the Supporting Information).

*4-N-Benzoyl-2′,3′-O-isopropylidenecytidine (**3**).* **3** was synthesized as previously described (see Scheme 1).[26,27]

*4-N-Benzoyl-2′,3′-O-isopropylidenecytidine-5′-tert-butylcarboxylate (**4**).* **4** was synthesized in a manner similar to a previous report.[28] **3** (1.92 g, 4.96 mmol, 1.0 equiv) was suspended in DCM (20 mL). To this solution were added pyridinium dichromate (PDC, 3.73 g, 9.91 mmol, 2.0 equiv), acetic anhydride (Ac_2O, 4.69 mL, 4.96 mmol, 10.0 equiv), and *tert*-butyl alcohol (*t*-BuOH, 9.48 mL, 99.1 mmol, 20.0 equiv) sequentially, and the mixture was stirred for 3 h. The reaction was diluted in an excess of EtOAc (400 mL), filtered through a pad of silica gel, and rinsed with excess EtOAc, and the solution was concentrated in vacuo. The residue was purified by chromatography on silica gel using a gradient of 0−100% EtOAc in hexanes to yield **4** as a light yellow foam (1.77 g, 3.87 mmol, 78% yield). ^{1}H NMR (500 MHz, $CDCl_3$): δ 9.08 (s, 1H), 8.01 (d, J = 7.4 Hz, 1H), 7.86 (d, J = 7.3 Hz, 2H), 7.56 (app t, J = 7.5 Hz, 1H), 7.51−7.37 (m, 3H), 5.71 (s, 1H), 5.28 (dd, J = 6.1, 2.1 Hz, 1H), 5.16 (d, J = 6.1 Hz, 1H), 4.61 (d, J = 2.0 Hz, 1H), 1.53 (s, 3H), 1.46 (s, 9H), 1.35 (s, 3H) ppm. ^{13}C NMR (126 MHz, $CDCl_3$): δ 168.3, 166.6, 162.8, 154.6, 148.0, 133.0, 128.8, 127.5, 113.2, 98.4, 96.6, 88.3, 84.6, 84.4, 82.4, 27.9, 26.5, 25.0 ppm. One carbon signal is merged into another; the possible merged peak is visible in the ^{13}C NMR of **3**, **5**, **7**, and **9** at approximately 132.9 ppm. HRMS-ESI$^+$ (m/z) calcd $[M + H]^+$ for $C_{23}H_{28}N_3O_7$: 458.1922; found: 458.1903.

*4-N-Benzoyl-3′-deoxy-3′,4′-didehydro-2′-O-tert-butyldimethylsilylcytidine-5′-tert-butylcarboxylate (**5**).* **5** was synthesized in a manner similar to a previous report.[23] **4** (6.55 g, 14.3 mmol, 1.0 equiv) was dissolved in *t*-BuOH (90 mL), and to this solution was added *t*-BuOK (3.37 g, 30.1 mmol, 2.0 equiv). The reaction was stirred until the starting material was observed to be consumed by TLC (approximately 5 min). The reaction was neutralized to approximately pH 7 with glacial acetic acid and then concentrated in vacuo. The reaction was dried on a high vacuum for at least 1 h before proceeding. The residue was then dissolved in DMF (50 mL), to this solution were added *tert*-butyldimethylsilyl chloride (TBSCl, 8.62 g, 57.2 mmol, 2.0 equiv) and imidazole (3.89 g, 57.2 mmol, 2.0 equiv), and the reaction was stirred for 30 min. The reaction was monitored by TLC to ensure reaction completion (if the reaction was incomplete, this indicates that residual *t*-BuOH is still present and excess TBSCl should be added until all starting material is converted). The reaction was then directly poured into a separatory funnel, diluted in a 1:1 mixture of EtOAc and hexanes (800 mL), and washed with 1 M aqueous HCl (300 mL), saturated aqueous $NaHCO_3$ (300 mL), and brine (300 mL). The organic layer was dried over Na_2SO_4, filtered, and concentrated in vacuo. The residue was purified by chromatography on silica gel using a gradient of 0−60% EtOAc in hexanes to yield **5** as a white foam (5.68 g, 11.1 mmol, 77% yield). ^{1}H NMR (500 MHz, $CDCl_3$): δ 8.83 (br s, 1H), 7.89 (d, J = 7.7 Hz, 2H), 7.59 (app t, J = 7.4 Hz, 1H), 7.56−7.46 (m, 4H), 6.28 (d, J = 2.2 Hz, 1H), 5.94 (d, J = 2.6 Hz, 1H), 5.03 (app t, J = 2.4 Hz, 1H), 1.55 (s, 9H), 0.89 (s, 9H), 0.16 (s, 3H), 0.10 (s, 3H) ppm. ^{13}C NMR (126 MHz, $CDCl_3$): δ 166.8, 162.6, 158.1, 154.0, 150.6, 143.6, 133.0, 132.8, 128.7, 127.6, 111.7, 97.0, 95.5, 83.2, 79.8, 27.8, 25.5, 17.9, −4.8, −5.0 ppm. HRMS-ESI$^+$ (m/z) calcd [M + H]$^+$ for $C_{26}H_{36}N_3O_6Si$: 514.2368; found: 514.2341.

*4-N-Benzoyl-3′-deoxy-3′,4′-didehydro-2′-O-tert-butyldimethylsilylcytidine (**7**).* **5** (700.0 mg, 1.36 mmol, 1.0 equiv) was dissolved in DCM (9 mL). To this solution was added NaOH (3 M solution in MeOH, 908 μL; the final solvent ratio is approximately 9:1 DCM:MeOH), and the solution was stirred until the mixture solidified into a gel-like solid (<1 to 30 min). The crude mixture was transferred to a separatory funnel, washed with 1 M aqueous HCl (300 mL), and extracted with EtOAc (600 mL; mix in a separatory funnel until the solid solubilizes), and the organic layer was dried over Na_2SO_4 and concentrated in vacuo. Crude 4-*N*-benzoyl-3′-deoxy-3′,4′-didehydro-2′-*O*-*tert*-butyldimethylsilylcytidine-5′-carboxylate (**6**, 537 mg, 1.21 mmol, 79% yield) was used without further purification. ^{1}H NMR (500 MHz, MeOD): δ 7.98 (d, J = 7.2 Hz, 2H), 7.87 (d, J = 7.5 Hz, 1H), 7.64 (app t, J = 7.4 Hz, 1H), 7.61 (d, J = 7.4 Hz, 1H), 7.54 (app t, J = 7.8 Hz, 2H), 6.32 (d, J = 2.4 Hz, 1H), 6.11 (d, J = 2.6 Hz, 1H), 5.20 (app t, J = 2.6 Hz, 1H), 0.94 (s, 9H), 0.18 (s, 3H), 0.15 (s, 3H) ppm. ^{13}C NMR (126 MHz, MeOD): δ 169.2, 165.3, 162.1, 157.4, 151.7, 145.7, 134.6, 134.2, 129.8, 129.2, 113.7, 99.0, 97.1, 81.5, 26.2, 18.9, −4.6, −4.7 ppm. HRMS-ESI$^+$ (m/z) calcd [M + H]$^+$ for $C_{22}H_{28}N_3O_6Si$: 458.1742; found: 458.1726.

Crude **6** was dissolved in THF (30 mL) and cooled to 0 °C, and to this solution were added ethyl chloroformate (393 μL, 4.11 mmol, 3.6 equiv) and triethylamine (261 μL, 1.87 mmol, 1.6 equiv). After reagent addition, the reaction was allowed to warm to room temperature and stirred for 2 h. After 2 h, the mixture was cooled to 0 °C. To the solution was added $NaBH_4$ (88.5 mg, 2.34 mmol, 2 equiv), then water (15 mL) was added dropwise over 30 min to fully dissolve all $NaBH_4$, and the reaction was stirred for an additional 1 h at 0 °C. The solution was then concentrated in vacuo, redissolved in EtOAc (300 mL), and washed with 1 M aqueous HCl (200 mL), saturated aqueous $NaHCO_3$ (200 mL), and brine (200 mL). The organic layer was then dried over Na_2SO_4 and concentrated in vacuo. The residue was purified by chromatography on silica gel using a gradient of 0−100% EtOAc in DCM to yield **7** as a white foam (226 mg, 0.509 mmol, 44% yield). ^{1}H NMR (500 MHz, $CDCl_3$): δ 9.18 (s, 1H), 7.81 (d, J = 7.2 Hz, 2H), 7.66 (d, J = 7.5 Hz, 1H), 7.52 (app t, J = 7.4 Hz, 1H), 7.46−7.33 (m, 3H), 6.34 (d, J = 1.5 Hz, 1H), 5.17 (d, J = 2.5 Hz, 1H), 4.81 (app t, J = 2.0 Hz, 1H), 4.34 (d, J = 14.2 Hz, 1H), 4.29 (d, J = 14.3 Hz, 1H), 0.85 (s, 9H), 0.10 (s, 3H), 0.05 (s, 3H) ppm. ^{13}C NMR (126 MHz, $CDCl_3$): δ 166.7, 162.6, 161.2, 154.7, 143.7, 133.0, 132.7, 128.8, 127.6, 101.3, 97.1, 94.0, 80.6, 57.2, 25.6, 18.0, −4.7, −4.9 ppm. HRMS-ESI$^+$ (m/z) calcd [M + H]$^+$ for $C_{22}H_{30}N_3O_5Si$: 444.1949; found: 444.1933.

*Isopropyl ((S)-(((4R,5R)-5-(4-Benzamido-2-oxopyrimidin-1(2H)-yl)-4-((tert-butyldimethylsilyl)oxy)-4,5-dihydrofuran-2-yl)methoxy)(phenoxy)phosphoryl)-L-alaninate (**8**).* **8** was synthesized utilizing a reported methodology.[30] **7** (153 mg, 0.345 mmol, 1.0 equiv) and *N*-[(*S*)-(2,3,4,5,6-pentafluorophenoxy)phenoxyphosphinyl]-L-alanine-1-isopropyl ester (234 mg, 0.517 mmol, 1.5 equiv) were mixed as dry powders in a flame-dried 10 mL round-bottom flask and vacuum-dried overnight before use. The reaction was backfilled with N_2, then dissolved in anhydrous pyridine (1.5 mL), and cooled to 0 °C. To this solution was added $AlMe_2Cl$ (1.0 M solution in hexanes, 173 μL, 0.173 mmol, 0.5 equiv), and the mixture was stirred at 0 °C for 10 min before warming to room temperature and stirring for 48 h at room temperature under N_2. The reaction was quenched by the addition of aqueous L-tartaric acid (30% w/v solution, 1 mL), the mixture was transferred to a separatory funnel, extracted with EtOAc (100 mL), and washed with brine (100 mL, 2×), and then the organic layer was dried over Na_2SO_4 and concentrated in vacuo. The residue was purified by chromatography on silica gel using a gradient of 0−60% EtOAc in hexanes to yield **8** as a light yellow oil (203 mg, 0.319 mmol, 93% yield). ^{1}H NMR (500 MHz, $CDCl_3$): δ 9.28 (br s, 1H), 7.93 (d, J = 7.5 Hz, 2H), 7.56 (app t, J = 7.4 Hz, 1H), 7.51 (d, J = 7.5 Hz, 1H), 7.46 (app t, J = 7.7 Hz, 2H), 7.43−7.33 (m, 1H), 7.30 (app t, J = 8.1 Hz, 2H), 7.22 (d, J = 8.5 Hz, 2H), 7.14 (app t, J = 7.3 Hz, 1H), 6.30 (d, J = 1.5 Hz, 1H), 5.19 (d, J = 2.4 Hz, 1H), 5.00 (hept, J = 6.2 Hz, 1H), 4.78 (s, 1H), 4.74 (s, 1H), 4.72 (s, 1H), 4.30 (q, J = 9.6 Hz, 1H), 4.01−3.91 (m, 1H), 1.41 (d, J = 7.1 Hz, 3H), 1.21 (d, J = 4.4 Hz, 3H), 1.20 (d, J = 4.3 Hz, 3H), 0.86 (s, 9H), 0.12 (s, 3H), 0.06 (s, 3H) ppm. ^{13}C NMR (126 MHz, $CDCl_3$): δ 172.8 (d, $J_{C\text{-}P}$ = 6.9 Hz, 1C), 166.5, 162.6, 156.3 (d, $J_{C\text{-}P}$ = 8.4 Hz, 1C), 154.2, 150.6 (d, $J_{C\text{-}P}$ = 6.8 Hz, 1C), 143.1, 133.0, 129.7, 128.7, 127.8, 125.0, 120.0 (d, $J_{C\text{-}P}$ = 4.9 Hz), 104.0, 97.0, 94.3, 80.4, 69.1, 60.5 (d, $J_{C\text{-}P}$ = 4.3 Hz, 1C), 50.3, 25.6, 21.6, 21.6, 20.6 (d, $J_{C\text{-}P}$ = 5.3 Hz, 1C), 18.0, −4.7, −5.0 ppm. One carbon signal is merged into another; possible merged peak is visible in the ^{13}C NMR of **3**, **5**, **7**, and **9** at approximately 132.9 ppm. ^{31}P NMR (202 MHz, $CDCl_3$): δ 2.69 ppm. HRMS-ESI$^+$ (m/z) calcd [M + H]$^+$ for $C_{34}H_{46}N_4O_9PSi$: 713.2766; found: 713.2739.

*Isopropyl ((S)-(((4R,5R)-5-(4-Benzamido-2-oxopyrimidin-1(2H)-yl)-4-hydroxy-4,5-dihydrofuran-2-yl)methoxy)(phenoxy)phosphoryl)-L-alaninate (**9**).* **8** (48.1 mg, 0.0755 mmol, 1.0 equiv) was dissolved in THF (1 mL) and aqueous CF_3CO_2H (80% CF_3CO_2H, v/v, 1 mL) and stirred for 3 h. The reaction was concentrated in vacuo and purified by chromatography on silica gel using a gradient of 0−10% MeOH in DCM to yield **9** as a colorless oil (23.5 mg, 0.0393 mmol, 52% yield). ^{1}H NMR (500 MHz, $CDCl_3$): δ 9.38 (br s, 1H), 7.91 (d, J = 7.3 Hz, 2H), 7.67 (d, J = 7.5 Hz, 1H), 7.56 (app t, J = 7.4 Hz, 1H), 7.54−7.49 (m, 1H), 7.45 (app t, J = 7.7 Hz, 2H), 7.31 (app t, J = 7.8 Hz, 2H), 7.21 (d, J = 8.1 Hz, 2H), 7.14 (app t, J = 7.4 Hz, 1H), 6.25 (d, J = 2.1 Hz, 1H), 5.32 (d, J = 2.4 Hz, 1H), 4.99 (hept, J = 6.3 Hz, 1H), 4.89 (s, 1H), 4.75 (s, 1H), 4.74 (s, 1H), 4.61 (br s, 1H), 4.19 (q, J = 9.7 Hz, 1H), 4.03−3.91 (m, 1H), 1.39 (d, J = 7.1 Hz, 3H), 1.21 (d, J = 1.7 Hz, 3H), 1.20 (d, J = 1.8 Hz, 3H) ppm. ^{13}C NMR (126 MHz, $CDCl_3$): δ 172.9 (d, $J_{C\text{-}P}$ = 7.1 Hz, 1C), 166.7, 162.8, 156.1 (d, $J_{C\text{-}P}$ = 8.2 Hz, 1C), 155.2, 150.5 (d, $J_{C\text{-}P}$ = 6.8 Hz, 1C), 143.1, 133.0, 132.9, 129.7, 128.8, 127.8, 125.0, 120.0 (d, $J_{C\text{-}P}$ = 4.9 Hz, 1C), 103.6, 97.2, 95.3, 80.0, 69.2, 60.5 (d, $J_{C\text{-}P}$ = 4.4 Hz, 1C), 50.3, 21.6, 21.6, 20.7 (d, $J_{C\text{-}P}$ = 5.3 Hz, 1C) ppm. ^{31}P NMR (202 MHz, $CDCl_3$): δ 2.69 ppm. HRMS-ESI$^+$ (m/z) calcd [M + H]$^+$ for $C_{28}H_{32}N_4O_9P$: 599.1901; found: 599.1878.

*Isopropyl ((S)-(((4R,5R)-5-(4-Amino-2-oxopyrimidin-1(2H)-yl)-4-hydroxy-4,5-dihydrofuran-2-yl)methoxy)(phenoxy)phosphoryl)-L-alaninate (**1**).* **9** (79.1 mg, 0.132 mmol, 1.0 equiv) was dissolved in acetic acid and pyridine (AcOH:pyridine, 1:4; 500 μL), to this flask was added hydrazine hydrate (64% NH_2NH_2, 30.0 μL, 0.396 mmol, 3.0 equiv), and the reaction was stirred for 24 h. The reaction was concentrated in vacuo and purified by chromatography on silica gel using a gradient of 0−15% MeOH in DCM to yield **1** as a pale yellow foam (55.8 mg, 0.113 mmol, 85% yield). The Harki laboratory identifier for **1** is HLB-0532247. ^{1}H NMR (500 MHz, $CDCl_3$): δ 7.35−7.25 (m, 3H), 7.21 (d, J = 8.1 Hz, 2H), 7.15 (app t, J = 7.4 Hz, 1H), 6.22 (s, 1H), 5.76 (d, J = 7.4 Hz, 1H), 5.28 (s, 1H), 5.00 (hept, J = 6.2 Hz, 1H), 4.90

(s, 1H), 4.70 (s, 1H), 4.69 (s, 1H), 4.13 (app t, J = 10.7 Hz, 1H), 4.01−3.90 (m, 1H), 1.37 (d, J = 7.0 Hz, 3H), 1.23 (d, J = 2.4 Hz, 3H), 1.21 (d, J = 2.4 Hz, 3H) ppm. ^{13}C NMR (126 MHz, $CDCl_3$): δ 173.2 (d, $J_{C\text{-}P}$ = 6.4 Hz, 1C), 166.0, 156.1, 156.0, 150.6 (d, $J_{C\text{-}P}$ = 6.7 Hz, 1C), 139.8, 129.7, 125.1, 120.1 (d, $J_{C\text{-}P}$ = 4.8 Hz, 1C), 103.5, 95.8, 94.8, 79.6, 69.3, 60.9, 50.4, 21.7, 21.6, 20.7 (d, $J_{C\text{-}P}$ = 5.6 Hz, 1C) ppm. ^{31}P NMR (202 MHz, $CDCl_3$): δ 2.64 ppm. HRMS-ESI$^+$ (m/z) calcd $[M + H]^+$ for $C_{21}H_{28}N_4O_8P$: 495.1639; found: 495.1617.

*4-N-Benzoyl-3′-deoxy-3′,4′-didehydro-2′-O-tert-butyldimethylsilylcytidine-5′-H-phosphonate (**10**; Scheme S1).* **10** was synthesized using a reported methodology.[43] **7** (106 mg, 0.239 mmol, 1.0 equiv) was vacuum-dried overnight before use. 2-Chloro-1,3,2-benzodioxaphosphorin-4-one (58.1 mg, 0.287 mmol, 1.2 equiv) was vacuum-dried overnight before use. 2-Chloro-1,3,2-benzodioxaphosphorin-4-one was dissolved in anhydrous dioxane and pyridine (1:1 v/v solution, 4 mL). To this solution was added a solution of **7** dissolved in anhydrous dioxane and pyridine (1:1, 1 mL), and the mixture was stirred at room temperature for 2 h. After 2 h, the reaction was quenched with H_2O (1 mL) and the mixture was evaporated in vacuo. The residue was purified by chromatography on Et_3N-deactivated silica gel using a gradient of 0−20% MeOH in DCM to yield **10** (triethylammonium salt) as a glassy solid (105 mg, 0.172 mmol, 72% yield). Loss of the TBS group can occur on acidic silica gel, which in this case also yielded 4-*N*-benzoyl-3′-deoxy-3′,4′-didehydrocytidine-5′-*H*-phosphonate (**11**, 26.4 mg, 0.0534 mmol, 22% yield). Spectral data for **10**: ^{1}H NMR (500 MHz, MeOD): δ 7.98 (d, J = 7.0 Hz, 2H), 7.93 (d, J = 7.6 Hz, 1H), 7.64 (m, J = 8.2 Hz, 2H), 7.54 (app t, J = 7.7 Hz, 2H), 6.86 (d, $J_{H\text{-}P}$ = 625 Hz, 1H), 6.30 (d, J = 1.4 Hz, 1H), 5.40 (d, J = 2.6 Hz, 1H), 4.92 (s, 1H), 4.60 (s, 1H), 4.58 (s, 1H), 3.21 (q, J = 7.3 Hz, 8H), 1.31 (t, J = 7.3 Hz, 12H), 0.92 (s, 9H), 0.18 (s, 3H), 0.13 (s, 3H) ppm. (Quartets at 3.47 and 3.20 and triplets at 1.35 and 1.31 ppm correspond to the triethylamine salt form of the product, as well as excess triethylamine-HCl in the product that was not removed in this preparation.) ^{13}C NMR (126 MHz, MeOD): δ 169.0, 165.1, 160.1 (d, $J_{C\text{-}P}$ = 7.7 Hz, 1C), 157.6, 145.2, 134.7, 134.1, 129.8, 129.2, 103.9, 98.9, 95.8, 82.0, 63.5, 59.2 (d, $J_{C\text{-}P}$ = 3.3 Hz, 1C), 53.6, 47.8, 26.2, 18.9, 9.2, 7.6, −4.5, −4.6 ppm. ^{31}P NMR (202 MHz, MeOD): δ 4.30 ppm. HRMS-ESI$^+$ (m/z) calcd $[M + Et_3N + H]^+$ for $C_{28}H_{46}N_4O_7PSi$: 609.2868; found: 609.2844.

*4-N-Benzoyl-3′-deoxy-3′,4′-didehydrocytidine-5′-H-phosphonate (**11**; Scheme S1).* **10** (870. mg, 1.43 mmol, 1.0 equiv) was dissolved in DMF (10 mL), and to this solution was added dropwise triethylamine trihydrofluoride ($Et_3N{\cdot}3HF$, 583 μL, 3.58 mmol, 2.5 equiv). The reaction was monitored by TLC until it was complete (approximately 3 h). The reaction was directly evaporated in vacuo, and the residue was purified by chromatography on silica gel using a gradient of 0−20% MeOH in DCM to yield **11** (triethylammonium salt) as a glassy colorless solid (436 mg, 0.882 mmol, 62% yield). ^{1}H NMR (500 MHz, MeOD): δ 7.97 (d, J = 7.5 Hz, 2H), 7.92 (d, J = 7.5 Hz, 1H), 7.67−7.60 (m, 2H), 7.54 (app t, J = 7.7 Hz, 2H), 6.85, (d, $J_{H\text{-}P}$ = 620 Hz, 1H), 6.33 (d, J = 1.5 Hz, 1H), 5.42 (d, J = 2.4 Hz, 1H), 4.80 (s, 1H), 4.58 (s, 1H), 4.57 (s, 1H), 3.47 (q, J = 7.3 Hz, 6H), 1.35 (t, J = 7.3 Hz, 9H). ^{13}C NMR (126 MHz, MeOD): δ 169.0, 165.1, 160.3 (d, $J_{C\text{-}P}$ = 7.4 Hz, 1C), 157.6, 145.2, 134.7, 134.1, 129.8, 129.2, 103.2, 98.9, 95.8, 80.5, 63.5, 59.1 (d, $J_{C\text{-}P}$ = 3.6 Hz, 1C), 53.6, 7.63 ppm. HRMS-ESI$^+$ (m/z) calcd [M + H; no salt form]$^+$ for $C_{16}H_{17}N_3O_7P$: 394.0799; found: 394.0786.

*3′-Deoxy-3′,4′-didehydrocytidine-5′-triphosphate (**ddhCTP**; Scheme S1).* **ddhCTP** was synthesized using a reported methodology.[43] **11** (78.2 mg, 0.158 mmol, 1.0 equiv) and a stir bar were vacuum-dried overnight in a flame-dried flask before use. Tri(tetrabutylammonium)pyrophosphate (TBAPP, 285 mg, 0.316 mmol, 2.0 equiv) was similarly vacuum-dried overnight in a flame-dried flask before use. **11** was then purged and flushed with nitrogen gas before dissolving in anhydrous DMF (1.5 mL) and anhydrous pyridine (318 μL, 3.95 mmol, 25 equiv). To this solution was added fresh distilled trimethylsilyl chloride (TMSCl, 100. μL, 0.790 mmol, 5 equiv; distilled as described in General Procedure), and the solution was stirred for 10 min. Solid I_2 (60.2 mg, 0.237 mmol, 1.5 equiv) was dissolved in anhydrous DMF (1 mL), this solution was added dropwise to the reaction mixture until a brown color persisted, and then the reaction was allowed to stir for an additional 5 min. TBAPP was dissolved in anhydrous DMF (1 mL), added all at once to the reaction mixture, and then stirred for 1 h. Next, the crude mixture was transferred to a sealed tube, $MeNH_2$ in EtOH (30% w/v, 3 mL) was added, the flask was sealed, and the mixture was stirred at 50 °C for 18 h behind a shield. The crude reaction mixture was cooled and concentrated in vacuo. A Sephadex LH-20 column (2.5 × 40 cm) was equilibrated with aqueous triethylammonium acetate (10 mM TEAA, pH 8) buffer. The crude reaction mixture was dissolved in the same buffer and transferred to the column, and the molecules were eluted at 2 mL/min with the same buffer (10 mM TEAA, pH 8). Fractions were frozen, lyophilized, and analyzed by ^{1}H and ^{31}P NMR. Fractions containing the product were further purified by preparative HPLC (column: Agilent Technologies Zorbax SB-C18; 21.2 × 250 mm size, 7 μm pore; method: solvent A, 10 mM TEAA (pH 7.5); solvent B, 1:1 solution of 10 mM TEAA (pH 7.5) and MeCN; gradient, 98:2 A:B from 0 to 5 min, followed by a linear gradient to 60:40 A:B from 5 to 30 min, and an isocratic 60:40 A:B from 30 to 35 min), and the pure lyophilized fractions were confirmed by NMR, combined, and then lyophilized. **ddhCTP** (tetratriethylammonium salt) was isolated as a glassy colorless solid (7.67 μmol, 5% yield, which was determined using UV−Vis spectrometry and Beer's law using the extinction coefficient for cytidine). ^{1}H NMR (500 MHz, D_2O): δ 7.49 (d, J = 7.5 Hz, 1H), 6.33 (d, J = 1.8 Hz, 1H), 6.06 (d, J = 7.6 Hz, 1H), 5.53 (d, J = 2.7 Hz, 1H), 4.90 (s, 1H), 4.74−4.65 (m, 2H), 3.21 (q, J = 7.3 Hz, 14H), 1.29 (t, J = 7.3 Hz, 20H) ppm. ^{31}P NMR (202 MHz, D_2O): δ −10.4 (d, J = 19.9 Hz), −11.4 (d, J = 19.8 Hz), −23.2 (t, J = 19.9 Hz) ppm. LRMS-ESI$^+$ (m/z) calcd $[M + H]^+$ for $C_9H_{15}N_3O_{13}P_3$: 466.0; found: 465.9. LRMS-ESI$^-$ (m/z) calcd $[M - H]^-$ for $C_9H_{13}N_3O_{13}P_3$: 464.0; found: 463.8.

General Cell Culture. All cell lines were maintained in a humidified 5% CO_2 environment at 37 °C. HUH7 and HUH7.5 cells (human hepatocyte-derived cells from carcinoma, Apath LLC, New York, NY, USA) were cultured in DMEM (4500 mg/L "high glucose" + L-glutamine + 25 mM HEPES−sodium pyruvate; 12430-062, Life Technologies) supplemented with fetal bovine serum (FBS, Gibco; 10% FBS was used for cytotoxicity assays and 2% FBS was used in antiviral plaque assays), penicillin (100 IU/mL), streptomycin (100 μg/mL), and 1% nonessential amino acids (NEAA; Sigma Aldrich M7145-100ML) at a density of 2 × 10^5 to 2 × 10^6 cells/mL. Vero cells (ATCC, CCL-81) were cultured in EMEM media (ATCC) supplemented with FBS (10% FBS was used for cytotoxicity assays and 2% FBS was used in antiviral plaque assays), penicillin (100 IU/mL), and streptomycin (100 μg/mL) at a density of 2 × 10^5 to 2 × 10^6 cells/mL. HUH7 cells were verified by short tandem repeat (STR) profiling by Creative Bioarray.

Antiviral Plaque Assay. DMSO stock solutions of ddhC and **1** were diluted into the appropriate cell media (0, 0.1, and 1 mM). Vero, HUH7, and HUH7.5 cells grown in 24-well plates were used to characterize differential antiviral responses by cell type. Twenty-four hours prior to confluency, cells were pretreated with compound-containing media (250 μL). After pretreatment, cells were checked for confluency, compound-containing media were removed, and viral dilutions of either West Nile virus (WNV, originally isolated from American Crow from Albany Co, NY, in 2003; Vero pass X2 + C6/36 pass X2; accession #DQ164189)[44] or Zika virus (ZIKV) PRABC59 were prepared. Plates were infected at an MOI of 0.1 with diluted virus (100 μL) for 1 h and rocked every 30 min to ensure even distribution. After inoculation, the inoculum was removed, and wells were washed three times with Hank's balanced salt solution (BA-1, 1 mL each time). Plates were then overlaid with the appropriate compound-containing media (1 mL) and were incubated at 37 °C with 5% CO_2 for either 3 days for WNV or 4 days for ZIKV. After incubation, cells were checked for cytopathic effect (to ensure infection) and contamination (to ensure purity). Medium aliquots (800 μL) were harvested from each well, stored in FBS (200 μL), and placed in a −80 °C freezer. Each concentration of each compound in all cell lines was tested in triplicate. Infectious virus was enumerated from stored samples using plaque titration as in ref 45. Titers were compared across compound concentrations using an ordinary one-way ANOVA with Dunnett's

multiple comparisons test. Samples that failed the Brown−Forsythe test were reanalyzed using a Welch ANOVA test and Dunnett's T3 multiple comparisons test using GraphPad Prism.

Western Blot of HINT1 in Vero and HUH7 Cells. HUH7 or Vero cells were grown to confluency in a T75 flask, detached using cell dissociation buffer (Gibco cat. #13151-014), collected by pelleting in a centrifuge at 1000 rpm, rinsed three times with cold PBS (10 mL), and pelleted using a centrifuge after each wash and decantation of the PBS solution. After decanting the last PBS wash, the cells were suspended in RIPA buffer (500 μL, Pierce cat. #89901) containing protease and nuclease inhibitors (tablets, Pierce cat. #32965). Cell lysates were stored at −80 °C until analysis. The cell protein concentration was normalized to the lowest concentration sample using a Thermo Scientific Pierce BSA Protein Assay, which was constructed according to the manufacturer's protocol. Normalized cell lysis samples were run on a 4−12% Bis-Tris gradient gel at 184 V, 0.38A, and 70 W for approximately 50 min. Samples were transferred using a Bio-Rad Trans-Blot Turbo system per manufacturer's instructions. Blocking was performed using a blocking solution (5%, Bio-Rad cat. #1706404) for 4 h at room temperature (the volume used was enough to cover the whole blot in a plastic container; approximately 10 mL was prepared). Blotting was performed using HINT1 polyclonal antibody (Proteintech, cat. #10717-1-AP; 1:500 dilution in 5% blocking solution with 1% sodium azide) for 18 h. The membrane was then washed five times with TBST (10 mL) for 5 min. Goat anti-rabbit 2° antibody (HRP conjugation, Bio-Rad, cat. #170-6515; 1:1000 dilution in 5% blocking solution with 1% sodium azide) was incubated for 2 h before HRP imaging. The membrane was washed five times with TBST (10 mL) for 5 min before reblotting for β-actin (Sigma Aldrich, cat. #A1978, 1:2000 dilution in 5% blocking solution with 1% sodium azide). A second series of washing with TBST (10 mL) for 5 min five times was followed by treatment with goat anti-mouse Alexa Fluor 680 antibody for imaging of β-actin as described above (Alexa Fluor Plus 680, Invitrogen, cat. #A32729, 1:1000 dilution in 5% blocking solution with 1% sodium azide). Imaging was performed on a LI-COR Odyssey FC as per manufacturer's instructions.

In Cellulo Metabolism of 1 and ddhC to ddhCTP. Mass spectrometry quantitation of prodrug metabolites was contracted to WuXi AppTec using cell samples and standards prepared by K.T.P. The cell culture collection procedure was based on a previous report.[46] HUH7 cells were seeded at 5×10^6 each into two T75 flasks in appropriate cell media (10 mL) and incubated for 24 h. A DMSO solution of **1** was diluted to yield a stock solution in media (1000 μM of **1** in 5% DMSO in media). An aliquot of media (1 mL) was removed from each of the T75 flasks, and then **1** (1 mL of the 1000 μM stock solution in 5% DMSO in media) was dosed to one flask (final concentration of **1** was 100 μM; final DMSO concentration was 0.5%). The second T75 flask received a negative, no-compound control (1 mL of 5% DMSO in media; resulting in a 0.5% final DMSO concentration), and both flasks were incubated for 24 h. After 24 h, the media were decanted from the flasks, and the cells were trypsinized (2 mL, Thermo Fisher), counted with an automated cell counter using Trypan blue stain (Thermo Fisher), and then centrifuged at 1000 rpm for 5 min. The pellets were resuspended in cold aqueous MeOH (60% MeOH, 1 mL), incubated at −20 °C overnight, and then the cells underwent three freeze−thaw cycles in liquid nitrogen. The cell mixture was centrifuged at 14,000 rpm for 5 min, and the supernatant was collected, lyophilized, and stored at −20 °C until use.

To analyze levels of **1** and **ddhCTP** found in lysates, the following procedure was employed. Lysate samples were reconstituted in a 1:1 solution of MeOH:H_2O (100 μL). An aliquot (4 μL) was treated with an internal standard solution (200 μL of 200 nM adenosine-$^{13}C_{10}$ 5′-triphosphate in MeOH; referred to as the internal standard (**IS**)), and the mixture was vortexed and then centrifuged at 3900 rpm for 10 min at 4 °C. An aliquot of the supernatant (100 μL) was further diluted with water (100 μL) in a sample plate, and then the plate was shaken at 800 rpm for 10 min. An aliquot of this mixture (20 μL) was injected for LC-MS analysis.

An identical procedure was performed for the culturing of cells and dosing of **ddhC**. To analyze levels of **ddhCTP** found in **ddhC**-dosed lysates, the previous procedure was employed. To analyze levels of **ddhC** found in lysates, the following procedure was employed. Cell lysates were reconstituted with cold aqueous MeOH (100 μL, 1:1 MeOH:H_2O). An aliquot (30 μL) was treated with a second internal standard solution (200 μL of 100 ng/mL adenosine $^{13}C_5$ in MeOH; referred to as internal standard 2 (**IS2**)), and the mixture was vortexed and then centrifuged at 12,000 rpm for 5 min at 4 °C. An aliquot of the resulting supernatant (180 μL) was blow-dried in a sample plate using nitrogen gas flow under 35 °C. The resulting residue was resuspended in water (150 μL) and shaken for 5 min, and aliquots of this solution (1 μL) were injected for LC-MS analysis. All cell lysate treatments were done in triplicate on different days paired with a DMSO control.

Sample concentrations of **1**, **ddhC**, and **ddhCTP** analytes were calculated by measuring the concentration of the analytes in three biological replicates for each compound dosed (**DMSO**, **1**, or **ddhC**) relative to a calibration curve of synthetic standards (see Figures S5−S7; see below for technical details). Concentrations of analytes measured are reported as nanomoles (nmol) detected per 5×10^6 cells in the collected lysates (cell counts and viabilities were measured during cell lysate collection using Trypan Blue staining).

Mass spectrometry data for the detection of **1** and **ddhCTP** were collected using a Sciex Triple Quad 6500 (ESI: negative; multiple reaction monitoring (MRM) detection of **ddhCTP** (464.2), **1** (493.1), and **IS** (516.3)) equipped with a Kentex EVO C18 column (2.6 μm, 20 × 2.1 mm). A two-solvent system was used as the eluents: solvent A, 5 mM *N*,*N*-dimethylhexylamine (DMHA) in water, pH 7; solvent B, 5 mM *N*,*N*-dimethylhexylamine (DMHA) in MeCN. The gradient (0.5000 mL/min flow rate) consisted of the following: 95:5 A:B from 0 to 0.1 min, followed by a linear gradient to 70:30 A:B from 0.1 to 2 min, and an isocratic 70:30 A:B from 2 to 2.70 min, followed by a return to the starting condition of 95:5 A:B from 2.70 to 2.71 min and a second isocratic 95:5 A:B from 2.71 to 3.50 min. Observed retention times of the standards were as follows: **ddhCTP**, 1.69 min; **1**, 2.31 min; **IS**, 1.75 min. A calibration curve of both **1** and **ddhCTP** was calculated by preparing a stock solution and diluting to form an eight-point dilution series from 1−3000 ng/mL (in PBS buffer) of the analyte standard along with 1 ng/mL **IS**. A plot of A_s/A_{IS} versus C_s/C_{IS} was made, and linear regression with $1/x^2$ weighing was performed to calculate a calibration curve where A_s is the analyte peak area, A_{IS} is the **IS** peak area, C_s is the concentration of the analyte, and C_{IS} is the concentration of the **IS**. Data analysis was performed using integrated Instrument Control and Data Processing Software Analyst 1.6.3 software. The experimental sample concentrations of **1** and **ddhCTP** were calculated based on these curves (see Figures S5 and S6). Final analyte concentrations are reported as the average of three replicates ± the standard deviation.

Mass spectrometry data for the detection of **ddhC** were collected using a Waters Zevo TQs LC-MS/MS system (ESI: positive; MRM detection of **ddhC** (226.1) and **IS2** (273.1)) equipped with an Acquity UPLC BEH C18 column (1.7 μm, 50 × 2.1 mm). A two-solvent system was used as the eluents: solvent A, 1% acetic acid in water, pH 8.5; solvent B, MeCN. The gradient (0.5000 mL/min flow rate) consisted of the following: 99:1 A:B from 0 to 0.90 min, followed by a linear gradient to 70:30 A:B from 0.90 to 1.30 min and a return to the starting condition of 95:1 A:B from 1.30 to 1.31 min, followed by an isocratic 99:1 A:B from 1.31 to 3.00 min. Observed retention times of the standards were as follows: **ddhC**, 0.75 min; **IS2**, 1.65 min. A calibration curve of **ddhC** and **IS2** was calculated by preparing a stock solution and diluting to form an eight-point dilution series from 5−2500 ng/mL **ddhC** standard (2:8 MeOH:H_2O, v/v) along with 1 ng/mL **IS2**. Curves using the analyte and **IS2** signal were prepared as above and used to calculate experimental sample concentrations of **ddhC** (see Figure S7). Final analyte concentrations are reported as the average of three replicates ± the standard deviation.

In the text, we made a note of approximating the molarity of cellular **ddhCTP** produced in the course of this dosing study. Approximate cell volumes and **ddhCTP** concentrations were calculated using previously published images of HUH7 cells to estimate the cell diameter,[39] and the cell volume was calculated using the formula $4/3 \times \pi \times r^3$, where r is an estimated 5 μm, giving an approximate cell volume of an HUH7 cell as

532 fL. Concentrations were then calculated after taking the measured amount of **ddhCTP** per sample and dividing it among the total number of cells collected at the end of the compound treatment.

Protocol for Alamar Blue Cell Viability Assay. Cytotoxicity assays were done similarly to those previously described.[47] HUH7 or Vero cells were seeded at a density of 2000 or 1500 cells/well, respectively, in the appropriate cell culture media (50 μL) in 96-well clear plates (Costar) and incubated for 24 h. A DMSO solution of **1** or **ddhC** was serially diluted in the appropriate cell line media, and each solution (50 μL) was dosed to the cells (well volume total of 100 μL; final DMSO concentration of 0.5%). DMSO-only and no-cell control wells were dosed with a DMSO−media solution (50 μL of 1% DMSO in media) rather than **1** or **ddhC**. The cells were then incubated for 2 or 5 days. Two hours before the designated time point, Alamar blue (10 μL, Invitrogen) was added to each well. At the time point, fluorescence data were measured using a BioTek Synergy H1 microplate reader. Cell viability was calculated by subtracting background fluorescence (no-cell control) from the measured fluorescence of each well. Wells with compounds were normalized to the DMSO-only control (100% viability) and no-cell controls. Each individual experiment was performed in groups of three technical replicates and then repeated at least in biological triplicate. The final cell viability percentage was calculated by averaging % viability from each of the biological replicates, and the uncertainty was calculated by propagating the standard deviations from each biological replicate (taking the square root of the sum of the squares of individual standard deviations). Cytotoxicity values were compared across drug concentrations using an ordinary one-way ANOVA with Dunnett's multiple comparisons test using GraphPad Prism and Microsoft Excel.

Caco-2 Cell Permeability Assays. Caco-2 permeability assays were contracted to WuXi AppTec using compounds synthesized by K.T.P. Caco-2 cells (ATCC HTB-37) were seeded at 1×10^5 cells/cm^2 onto polyethylene membranes (PET) in 96-well plates, and the medium was refreshed every 4−5 days until confluent monolayers formed (21−28 days). Transport solutions were prepared as follows: HBSS (Hank's balanced salt solution), 10 mM HEPES (pH 7.4), and test compound (2 μM or 10 μM of either **ddhC** or **1**), where the final DMSO concentration was <1%. Digoxin was used as a bidirectional assay control (2 μM); nadolol and metoprolol were tested at 2 μM in the apical (A) to basolateral (B) direction only. Cell monolayers were incubated with the corresponding transport solutions for 2 h in a humidified incubator set to 37 °C at 5% CO_2. After 2 h, samples of starting solution, donor solution, and receiver solution were quantified for each tested and control compound using LC-MS by analyzing peak area ratios of the different analytes relative to an internal standard that was added before analysis. At the end of each assay, Lucifer yellow rejection assays were performed to certify Caco-2 cell monolayer integrity. The apparent permeability coefficient P_{app} (cm/s) was then calculated using eq 1:

$$P_{app} = \frac{\left(\frac{dC_r}{dt}\right) \times V_r}{A \times C_0} \quad (1)$$

where dC_r/dt is the cumulative concentration of the compound in the chosen receiving chamber as a function of time (μM/s), V_r is the volume of the chosen chamber solution (0.075 mL, apical side; 0.25 mL, basolateral side), A is the surface area of the cell monolayer (0.0804 cm^2), and C_0 is the initial concentration of the compound in the donor chamber in μM. The efflux ratio was calculated by eq 2:

$$\text{efflux ratio} = \frac{P_{app}(BA)}{P_{app}(AB)} \quad (2)$$

where P_{app} (AB) is the permeability coefficient for the direction A to B, and P_{app} (BA) is the permeability coefficient for the direction B to A.

Human and Mouse Plasma Stability Assay. Plasma stability experiments were contracted to WuXi AppTec using prodrug **1** prepared by K.T.P. Pooled plasma samples (mouse: 20 males, from BioreclamationIVT, cat. #MSE00PLK2P2N, batch MSE321336; human: 3 male, 3 female from BioreclamationIVT, cat. #HUMANPLK2P2N, batch HMN51524) were thawed at 37 °C and centrifuged at 4000 rpm for 5 min, and clots were removed. pH was adjusted to 7.4 if necessary. **1** was diluted in DMSO (to 100 μM), and the positive control propantheline was diluted (to 100 μM) in a solution of aqueous MeOH (45% MeOH). Plasma solutions (98 μL) were dosed with the prepared solutions of test and control compounds to make a final 2 μM dose. Samples were then incubated at 37 °C in a water bath, and time points were taken at 0, 10, 30, 60, and 120 min. Time point samples were mixed with a quench solution containing internal standards tolbutamide (200 ng/mL) and labetalol (200 ng/mL) in a 1:1 solution of MeCN:MeOH. Quenched samples were centrifuged at 4000 rpm for 10 min before being subject to LC-MS. The amount of sample was quantified by the peak analyte ratio (PAR) relative to internal standards according to eq 3:

$$\%\ \text{remaining} = \frac{\text{PAR}(t_n)}{\text{PAR}(t_0)} \quad (3)$$

where the PAR(t_n) is the PAR measured at time t = 0, 10, 30, 60, or 120 min, and PAR(t_0) is the PAR measured at t = 0 min.

Simulated Gastric Fluid Stability Assay. SGF stability experiments were contracted to WuXi AppTec using prodrug **1** prepared by K.T.P. Simulated gastric fluid (SGF) was prepared by the dissolution of NaCl (0.08 g), pepsin (0.128 g), HCl (0.28 mL), and H_2O (40 mL), after which the pH is approximately 1.20. A 96-well plate was prepared by the addition of the chosen compound solution (2 μL; DMSO stock at 200 μM) to each of the wells corresponding to time points 0, 60, 120, 360, and 1440 min. SGF solution (198 μL) was added to each well except at the 0 time point, and the samples were incubated at 37 °C and shaken at 300 rpm for the appropriate time. When the time point was reached, the sample was mixed with 400 μL of cold MeCN containing internal standards (200 ng/mL tolbutamide and labetalol). All samples were centrifuged at 4000 rpm at 4 °C for 20 min, and aliquots were prepared for LC-MS-MS analysis. The remaining compound was measured as per eq 3.

Enzymatic Incorporation of ddhCTP by Human DNA Polymerase γ. Equimolar amounts of the template and FAM-labeled primer (see Figure 3A) were diluted in 1× annealing buffer (5 mM $Mg(OAc)_2$ and 20 mM HEPES (pH 7.5) in DNase/RNase free water) and heated to 95 °C for 10 min. The heat was then turned off, and the DNA was allowed to cool to room temperature overnight for complete annealing. Extension reaction mixtures were performed by combining DNA polymerase γ (10 nM), primer/template DNA-annealed duplex (100 nM), and 100 μM CTP, dCTP, or **ddhCTP** in reaction buffer (50 mM Tris-HCl, 100 mM KCl, 10 mM $MgCl_2$, 0.4 mg/mL BSA, and 15% glycerol). After the components were mixed, the assay was run at 37 °C and samples were taken at the indicated times: 0 (taken before addition of the nucleotide), 10, and 20 min. Time point samples were stored in aqueous quenching buffer (80% v/v formamide, 0.1 M EDTA, 0.01% w/v bromophenol blue, and 0.1% w/v xylene cyanol). Samples were then directly run on a 7 M 20% urea polyacrylamide gel and run for approximately 2.5 h until the substrate and product bands were separated on the single-nucleotide level. Gels were imaged using a Bio-Rad ChemiDoc. DNA sequences were purchased from Eurogentec. DNA polymerase γ (catalytic subunit, cat. #85) was purchased from Enzymax (Lexington, KY). Nucleotides CTP and dCTP were purchased from Thermo Fisher Scientific. The **ddhCTP** sample was synthesized as described in Experimental Section.

Construction of ZIKV RdRp Bacterial Expression Plasmid. The ZIKV RdRp (NS5 gene) was cloned into the pET26Ub-CHIS bacterial expression plasmid using a similar procedure as described for WNV RdRp (NS5 gene).[41] This system allows for the production of ubiquitin fusion proteins containing a carboxy-terminal hexahistidine tag that are then co- and/or post-translationally processed by the ubiquitin protease coexpressed from a second plasmid, pUBPS.[48,49] Briefly, the ZIKV RdRp coding region was amplified using a synthetic NS5 gene construct as a template (synthesized by GenScript) based upon the NS5 amino acid sequence of the Zika virus strain BeH815744 (AMA12087.1), oligonucleotides 5′-TGGTCCTGCGTCTCCGCGGTGGAGGTGGCGGTACCGGCGAAACCCTGGGC-3′ and 5′-GGTG-

ACCAGAGGATCCCAGAACGCCCGGGGTGCT-3′. The PCR product ZIKV RdRp was gel-purified and cloned into the pET26Ub-CHIS plasmid using SacII and BamHI sites. The final construct (pET26Ub-ZIKV-RdRp-CHIS) was confirmed by sequencing at The Pennsylvania State University's Nucleic Acid Facility.

Expression and Purification of ZIKV RdRp. ZIKV RdRp was expressed and purified using the same procedure reported for WNV RdRp.[41] Briefly, expression was performed at 15 °C by autoinduction, and cells were harvested, lysed by French press, and subjected to PEI precipitation followed by AMS04 precipitation, Ni-NTA chromatography, gel filtration, and protein concentration using Vivaspin concentrators.

ZIKV RdRp-Catalyzed Nucleotide Incorporation Assays. To assemble ZIKV RdRp elongation-competent complexes, purified ZIKV RdRp (1 μM) was mixed with a pGGC RNA primer (10 μM), RNA template (5′-UUUAGCUCUUCCUCUUUGCC-3′, 1 μM), ATP (10 μM), GTP (10 μM), and [α-^{32}P]-ATP (0.1 μCi/μL) for 30 min at 30 °C in the reaction buffer (50 mM HEPES (pH 7.5), 20 mM NaCl, 5 mM $MgCl_2$, and 10 mM 2-mercaptoethanol). For single-nucleotide incorporation assays, elongation complexes were assembled, and reactions were initiated with either 100 μM CTP, 3′-dCTP, or **ddhCTP** substrate and allowed to proceed for 5 min before being quenched with EDTA (50 mM). For chain termination experiments, reactions were allowed to proceed for an additional 1 min in the presence of the next correct nucleotide substrate (10 μM UTP) before being quenched. To evaluate the ability of **ddhCTP** or 3′-dCTP to inhibit RdRp elongation, elongation complexes were assembled, and reactions were initiated with the addition of UTP and CTP and varying concentrations of **ddhCTP** and allowed to proceed for 5 min before being quenched with EDTA (50 mM). Products were resolved from substrates by denaturing PAGE. ZIKV RdRp was diluted immediately prior to use in enzyme dilution buffer (50 mM HEPES (pH 7.5), 10 mM 2-mercaptoethanol, and 20% glycerol). The volume of the enzyme added to any reaction was always less than or equal to 1/10 of the total volume.

Denaturing PAGE Analysis of Polymerase-Catalyzed Reaction Products. Two volumes of loading buffer (10 μL of 90% formamide, 0.025% bromophenol blue, and 0.025% xylene cyanol) was added to quenched reaction mixtures (5 μL) and heated to 90 °C for 2–5 min prior to loading (5 μL) on a denaturing 23% polyacrylamide gel containing 1× TBE (89 mM Tris base, 89 mM boric acid, and 2 mM EDTA) and urea (7 M). Formamide gels contained an additional 20% formamide. Electrophoresis was performed in 1× TBE at 90 W. Gels were visualized by using a PhosphorImager (GE) and quantified by using ImageQuant TL software (GE).

■ ASSOCIATED CONTENT

Supporting Information

The Supporting Information is available free of charge at https://pubs.acs.org/doi/10.1021/acs.jmedchem.1c01481.

Supplementary figures (Figures S1–S7) and reaction scheme (Scheme S1); NMR spectroscopy data and HPLC chromatograms for synthesized compounds (PDF)

■ AUTHOR INFORMATION

Corresponding Author

Daniel A. Harki − *Department of Medicinal Chemistry, University of Minnesota, Minneapolis, Minnesota 55455, United States;* orcid.org/0000-0001-5950-931X; Email: daharki@umn.edu

Authors

Kellan T. Passow − *Department of Medicinal Chemistry, University of Minnesota, Minneapolis, Minnesota 55455, United States*

Haley S. Caldwell − *Department of Biomedical Sciences, State University of New York at Albany School of Public Health, Albany, New York 12144, United States; The Arbovirus Laboratory, Wadsworth Center, New York State Department of Health, Slingerlands, New York 12201, United States*

Kiet A. Ngo − *The Arbovirus Laboratory, Wadsworth Center, New York State Department of Health, Slingerlands, New York 12201, United States*

Jamie J. Arnold − *Department of Biochemistry and Molecular Biology, The Pennsylvania State University, University Park, Pennsylvania 16802, United States;* Present Address: Present address: Department of Microbiology and Immunology, University of North Carolina School of Medicine, Chapel Hill, North Carolina 27599, United States (J.J.A., C.E.C.)

Nicole M. Antczak − *Department of Health Sciences and Technology, ETH Zürich, Zürich 8092, Switzerland;* Present Address: Present address: Department of Chemistry, Skidmore College, Saratoga Springs, New York 12866, United States (N.M.A.)

Anoop Narayanan − *Department of Biochemistry and Molecular Biology, The Pennsylvania State University, University Park, Pennsylvania 16802, United States*

Joyce Jose − *Department of Biochemistry and Molecular Biology and Huck Institutes of the Life Sciences, The Pennsylvania State University, University Park, Pennsylvania 16802, United States*

Shana J. Sturla − *Department of Health Sciences and Technology, ETH Zürich, Zürich 8092, Switzerland*

Craig E. Cameron − *Department of Biochemistry and Molecular Biology, The Pennsylvania State University, University Park, Pennsylvania 16802, United States;* Present Address: Present address: Department of Microbiology and Immunology, University of North Carolina School of Medicine, Chapel Hill, North Carolina 27599, United States (J.J.A., C.E.C.)

Alexander T. Ciota − *Department of Biomedical Sciences, State University of New York at Albany School of Public Health, Albany, New York 12144, United States; The Arbovirus Laboratory, Wadsworth Center, New York State Department of Health, Slingerlands, New York 12201, United States*

Complete contact information is available at: https://pubs.acs.org/10.1021/acs.jmedchem.1c01481

Notes

The authors declare no competing financial interest.

■ ACKNOWLEDGMENTS

We gratefully acknowledge NIH R01-GM110129 (D.A.H.), R21-AI146856 (A.T.C.), and R01-AI045818 (C.E.C. and J.J.A.), as well as a Grant-in-Aid from the Office of the Vice President for Research, University of Minnesota, for financial support. Mass spectrometry was performed at the Analytical Biochemistry core facility of the University of Minnesota Masonic Cancer Center, which is supported by NIH P30-CA77598.

■ ABBREVIATIONS

Ac_2O, acetic anhydride; CTP, cytidine triphosphate; DCM, dichloromethane; **ddhC**, 3′-deoxy-3′,4′-didehydro-cytidine; **ddhCTP**, 3′-deoxy-3′,4′-didehydro-cytidine-5′-triphosphate; DENV, dengue virus; DMF, *N*,*N*′-dimethylformamide; DMP, 2,2-dimethoxypropane; EtOAc, ethyl acetate; FAM, carboxy

fluorescein; HINT1, histidine triad nucleotide-binding protein 1; HCV, hepatitis C virus; IFNα, interferon α; MeCN, acetonitrile; MeOH, methanol; NTP, nucleotide triphosphate; PDC, pyridinium dichromate; PV, polio virus; ProTide, phosphoramidate monophosphate prodrug; RdRp, RNA dependent RNA polymerase; RNA, ribonucleic acid; rPol, RNA polymerase; RT, reverse transcriptase; SARS-CoV-2, Severe Acute Respiratory Syndrome Coronavirus 2; SGF, simulated gastric fluid; TBAPP, tri(tetrabutylammonium)-pyrophosphate; *t*-BuOH, *tert*-butyl alcohol; *t*-BuOK, potassium *tert*-butoxide; TBSCl, *tert*-butyldimethylsilyl chloride; TEAA, triethylammonium acetate; TEA or Et_3N, triethylamine; TFA or CF_3CO_2H, trifluoroacetic acid; THF, tetrahydrofuran; TMSCl, trimethylsilyl chloride; WNV, West Nile virus; ZIKV, Zika virus

REFERENCES

(1) De Clercq, E.; Li, G. Approved Antiviral Drugs over the Past 50 Years. *Clin. Microbiol. Rev.* **2016**, *29*, 695.

(2) Gizzi, A. S.; Grove, T. L.; Arnold, J. J.; Jose, J.; Jangra, R. K.; Garforth, S. J.; Du, Q.; Cahill, S. M.; Dulyaninova, N. G.; Love, J. D.; Chandran, K.; Bresnick, A. R.; Cameron, C. E.; Almo, S. C. A Naturally Occurring Antiviral Ribonucleotide Encoded by the Human Genome. *Nature* **2018**, *558*, 610.

(3) Seifert, M.; Bera, S. C; van Nies, P.; Kirchdoerfer, R. N; Shannon, A.; Le, T.-T.-N.; Meng, X.; Xia, H.; Wood, J. M; Harris, L. D; Papini, F. S; Arnold, J. J; Almo, S.; Grove, T. L; Shi, P.-Y.; Xiang, Y.; Canard, B.; Depken, M.; Cameron, C. E; Dulin, D. Inhibition of SARS-CoV-2 Polymerase by Nucleotide Analogs: A Single Molecule Perspective. *eLife* **2021**, DOI: 10.7554/eLife.70968.

(4) McGuigan, C.; Pathirana, R. N.; Mahmood, N.; Hay, A. J. Aryl Phosphate Derivates of AZT Inhibit HIV Replication in Cells Where the Nucleoside is Poorly Active. *Bioorg. Med. Chem. Lett.* **1992**, *2*, 701.

(5) Mehellou, Y.; Rattan, H. S.; Balzarini, J. The ProTide Prodrug Technology: From the Concept to the Clinic. *J. Med. Chem.* **2018**, *61*, 2211.

(6) Alanazi, A. S.; James, E.; Mehellou, Y. The ProTide Prodrug Technology: Where Next? *ACS Med. Chem. Lett.* **2019**, *10*, 2.

(7) Serpi, M.; Pertusati, F. An Overview of Protide Technology and Its Implications to Drug Discovery. *Expert Opin. Drug Discovery* **2021**, *16*, 1149.

(8) Balzarini, J.; Cooney, D. A.; Dalal, M.; Kang, G. J.; Cupp, J. E.; De Clercq, E.; Broder, S.; Johns, D. G. 2′,3′-Dideoxycytidine: Regulation of Its Metabolism and Antiretroviral Potency by Natural Pyrimidine Nucleosides and by Inhibitors of Pyrimidine Nucleotide Synthesis. *Mol. Pharmacol.* **1987**, *32*, 798.

(9) Eriksson, S.; Kierdaszuk, B.; Munch-Petersen, B.; Oberg, B.; Johansson, N. G. Comparison of the Substrate Specificities of Human Thymidine Kinase 1 and 2 and Deoxycytidine Kinase toward Antiviral and Cytostatic Nucleoside Analogs. *Biochem. Biophys. Res. Commun.* **1991**, *176*, 586.

(10) Sofia, M. J.; Bao, D.; Chang, W.; Du, J.; Nagarathnam, D.; Rachakonda, S.; Reddy, P. G.; Ross, B. S.; Wang, P.; Zhang, H.-R.; Bansal, S.; Espiritu, C.; Keilman, M.; Lam, A. M.; Steuer, H. M. M.; Niu, C.; Otto, M. J.; Furman, P. A. Discovery of a β-D-2′-Deoxy-2′-α-Fluoro-2′-β-C-Methyluridine Nucleotide Prodrug (PSI-7977) for the Treatment of Hepatitis C Virus. *J. Med. Chem.* **2010**, *53*, 7202.

(11) Murakami, E.; Tolstykh, T.; Bao, H.; Niu, C.; Steuer, H. M. M.; Bao, D.; Chang, W.; Espiritu, C.; Bansal, S.; Lam, A. M.; Otto, M. J.; Sofia, M. J.; Furman, P. A. Mechanism of Activation of PSI-7851 and Its Diastereoisomer PSI-7977. *J. Biol. Chem.* **2010**, *285*, 34337.

(12) Saboulard, D.; Naesens, L.; Cahard, D.; Salgado, A.; Pathirana, R.; Velazquez, S.; McGuigan, C.; De Clercq, E.; Balzarini, J. Characterization of the Activation Pathway of Phosphoramidate Triester Prodrugs of Stavudine and Zidovudine. *Mol. Pharmacol.* **1999**, *56*, 693.

(13) Lee, W. A.; He, G.-X.; Eisenberg, E.; Cihlar, T.; Swaminathan, S.; Mulato, A.; Cundy, K. C. Selective Intracellular Activation of a Novel Prodrug of the Human Immunodeficiency Virus Reverse Transcriptase Inhibitor Tenofovir Leads to Preferential Distribution and Accumulation in Lymphatic Tissue. *Antimicrob. Agents Chemother.* **2005**, *49*, 1898.

(14) Ruane, P. J.; DeJesus, E.; Berger, D.; Markowitz, M.; Bredeek, U. F.; Callebaut, C.; Zhong, L.; Ramanathan, S.; Rhee, M. S.; Fordyce, M. W.; Yale, K. Antiviral Activity, Safety, and Pharmacokinetics/Pharmacodynamics of Tenofovir Alafenamide as 10-Day Monotherapy in HIV-1-Positive Adults. *JAIDS* **2013**, *63*, 449.

(15) Siddiqui, A. Q.; McGuigan, C.; Ballatore, C.; Zuccotto, F.; Gilbert, I. H.; De Clercq, E.; Balzarini, J. Design and Synthesis of Lipophilic Phosphoramidate d4T-MP Prodrugs Expressing High Potency against HIV in Cell Culture: Structural Determinants for in Vitro Activity and QSAR. *J. Med. Chem.* **1999**, *42*, 4122.

(16) Eisenberg, E. J.; He, G.-X.; Lee, W. A. Metabolism of GS-7340, a Novel Phenyl Monophosphoramidate Intracellular Prodrug of PMPA, in Blood. *Nucleos. Nucleot. Nucl.* **2001**, *20*, 1091.

(17) Murakami, E.; Wang, T.; Park, Y.; Hao, J.; Lepist, E.-I.; Babusis, D.; Ray, A. S. Implications of Efficient Hepatic Delivery by Tenofovir Alafenamide (GS-7340) for Hepatitis B Virus Therapy. *Antimicrob. Agents Chemother.* **2015**, *59*, 3563.

(18) Brinkman, K.; Kakuda, T. N. Mitochondrial Toxicity of Nucleoside Analogue Reverse Transcriptase Inhibitors: A Looming Obstacle for Long-Term Antiretroviral Therapy? *Curr. Opin. Infect. Dis.* **2000**, *13*, 5.

(19) Young, M. J. Off-Target Effects of Drugs That Disrupt Human Mitochondrial DNA Maintenance. *Front. Mol. Biosci.* **2017**, *4*, 74.

(20) Johnson, A. A.; Ray, A. S.; Hanes, J.; Suo, Z. C.; Colacino, J. M.; Anderson, K. S.; Johnson, K. A. Toxicity of Antiviral Nucleoside Analogs and the Human Mitochondrial DNA Polymerase. *J. Biol. Chem.* **2001**, *276*, 40847.

(21) Lim, S. E.; Copeland, W. C. Differential Incorporation and Removal of Antiviral Deoxynucleotides by Human DNA Polymerase γ. *J. Biol. Chem.* **2001**, *276*, 23616.

(22) Nagpal, K. L.; Horwitz, J. P. Nucleosides. XIV. Synthesis of 3′-Deoxyadenosine and 9-(3-Deoxy-α-L-Threo-Pentofuranosyl)Adenine. *J. Org. Chem.* **1971**, *36*, 3743.

(23) Boojamra, C. G.; Lemoine, R. C.; Lee, J. C.; Léger, R.; Stein, K. A.; Vernier, N. G.; Magon, A.; Lomovskaya, O.; Martin, P. K.; Chamberland, S.; Lee, M. D.; Hecker, S. J.; Lee, V. J. Stereochemical Elucidation and Total Synthesis of Dihydropacidamycin D, a Semisynthetic Pacidamycin. *J. Am. Chem. Soc.* **2001**, *123*, 870.

(24) Zemlicka, J.; Freisler, J. V.; Gasser, R.; Horwitz, J. P. Nucleosides. XVI. The Synthesis of 2′,3′-Dideoxy-3′,4′-Didehydro Nucleosides. *J. Org. Chem.* **1973**, *38*, 990.

(25) Lichtenthaler, F. W.; Kitahara, K.; Strobel, K. Nucleosides, XXIII. A simple Access to 3′-Aminoxylo-Nucleosides and 3′,4′-Unsaturated Purine Nucleosides. *Synthesis* **1974**, *1974*, 860.

(26) Misra, A.; Mishra, S.; Misra, K. Synthesis and Fluorescence Studies of Multiple Labeled Oligonucleotides Containing Dansyl Fluorophore Covalently Attached at 2′-Terminus of Cytidine Via Carbamate Linkage. *Bioconjugate Chem.* **2004**, *15*, 638.

(27) Jones, G. H.; Taniguchi, M.; Tegg, D.; Moffatt, J. G. 4′-Substituted Nucleosides. 5. Hydroxymethylation of Nucleoside 5′-Aldehydes. *J. Org. Chem.* **1979**, *44*, 1309.

(28) Corey, E. J.; Samuelsson, B. One-Step Conversion of Primary Alcohols in the Carbohydrate Series to the Corresponding Carboxylic *tert*-Butyl Esters. *J. Org. Chem.* **1984**, *49*, 4735.

(29) Classon, B.; Samuelsson, B. Synthesis of 5-Iodo-1-(Sodium 2-Deoxy-β-D-Ribofuranosyluronate)Uracil and 5-Iodo-1-(Sodium β-D-Ribofuranosyluronate)Uracil. *Acta Chem. Scand. B* **1985**, *39b*, 501.

(30) Simmons, B.; Liu, Z.; Klapars, A.; Bellomo, A.; Silverman, S. M. Mechanism-Based Solution to the ProTide Synthesis Problem: Selective Access to Sofosbuvir, Acelarin, and INX-08189. *Org. Lett.* **2017**, *19*, 2218.

(31) Letsinger, R. L.; Miller, P. S.; Grams, G. W. Selective N-Debenzoylation of N,O-Polybenzoylnucleosides. *Tetrahedron Lett.* **1968**, *9*, 2621.

(32) Petrová, M.; Buděšínský, M.; Rosenberg, I. Straightforward Synthesis of 3′-Deoxy-3′,4′-Didehydronucleoside-5′-Aldehydes Via 2′,3′-*O*-Orthoester Group Elimination: A Simple Route to 3′,4′-Didehydronucleosides. *Tetrahedron Lett.* **2010**, *51*, 6874.
(33) Dragoni, F.; Boccuto, A.; Picarazzi, F.; Giannini, A.; Giammarino, F.; Saladini, F.; Mori, M.; Mastrangelo, E.; Zazzi, M.; Vicenti, I. Evaluation of Sofosbuvir Activity and Resistance Profile against West Nile Virus in Vitro. *Antiviral Res.* **2020**, *175*, 104708.
(34) Mumtaz, N.; Jimmerson, L. C.; Bushman, L. R.; Kiser, J. J.; Aron, G.; Reusken, C. B. E. M.; Koopmans, M. P. G.; van Kampen, J. J. A. Cell-Line Dependent Antiviral Activity of Sofosbuvir against Zika Virus. *Antiviral Res.* **2017**, *146*, 161−163.
(35) Sun, J.; Yogarajah, T.; Lee, R. C. H.; Kaur, P.; Inoue, M.; Tan, Y. W.; Chu, J. J. H. Drug Repurposing of Pyrimidine Analogs as Potent Antiviral Compounds against Human Enterovirus A71 Infection with Potential Clinical Applications. *Sci. Rep.* **2020**, *10*, 8159.
(36) Sacramento, C. Q.; de Melo, G. R.; de Freitas, C. S.; Rocha, N.; Hoelz, L. V. B.; Miranda, M.; Fintelman-Rodrigues, N.; Marttorelli, A.; Ferreira, A. C.; Barbosa-Lima, G.; Abrantes, J. L.; Vieira, Y. R.; Bastos, M. M.; de Mello Volotão, E.; Nunes, E. P.; Tschoeke, D. A.; Leomil, L.; Loiola, E. C.; Trindade, P.; Rehen, S. K.; Bozza, F. A.; Bozza, P. T.; Boechat, N.; Thompson, F. L.; de Filippis, A. M. B.; Brüning, K.; Souza, T. M. L. The Clinically Approved Antiviral Drug Sofosbuvir Inhibits Zika Virus Replication. *Sci. Rep.* **2017**, *7*, 40920.
(37) Chou, T.-F.; Bieganowski, P.; Shilinski, K.; Cheng, J.; Brenner, C.; Wagner, C. R. ^{31}P NMR and Genetic Analysis Establish HINT as the Only *Escherchia Coli* Purine Nucleoside Phosphoramidase and as Essential for Growth under High Salt Conditions. *J. Biol. Chem.* **2005**, *280*, 15356.
(38) Blais, D. R.; Lyn, R. K.; Joyce, M. A.; Rouleau, Y.; Steenbergen, R.; Barsby, N.; Zhu, L.-F.; Pegoraro, A. F.; Stolow, A.; Tyrrell, D. L.; Pezacki, J. P. Activity-Based Protein Profiling Identifies a Host Enzyme, Carboxylesterase 1, Which Is Differentially Active During Hepatitis C Virus Replication. *J. Biol. Chem.* **2010**, *285*, 25602.
(39) Sainz, B., Jr.; TenCate, V.; Uprichard, S. L. Three-Dimensional Huh7 Cell Culture System for the Study of Hepatitis C Virus Infection. *Virol. J.* **2009**, *6*, 103.
(40) Wood, J. M.; Evans, G. B.; Grove, T. L.; Almo, S. C.; Cameron, S. A.; Furneaux, R. H.; Harris, L. D. Chemical Synthesis of the Antiviral Nucleotide Analogue ddhCTP. *J. Org. Chem.* **2021**, *86*, 8843.
(41) Van Slyke, G. A.; Arnold, J. J.; Lugo, A. J.; Griesemer, S. B.; Moustafa, I. M.; Kramer, L. D.; Cameron, C. E.; Ciota, A. T. Sequence-Specific Fidelity Alterations Associated with West Nile Virus Attenuation in Mosquitoes. *PLoS Pathog.* **2015**, *11*, e1005009.
(42) Armarego, W. L. F.; Chai, C. L. L. *Purification of Laboratory Chemicals*; 6th Ed.; Elsevier/Butterworth-Heinemann: Amsterdam, Boston, 2009; p xvi.
(43) Sun, Q.; Edathil, J. P.; Wu, R.; Smidansky, E. D.; Cameron, C. E.; Peterson, B. R. One-Pot Synthesis of Nucleoside 5′-Triphosphates from Nucleoside 5′-*H*-Phosphonates. *Org. Lett.* **2008**, *10*, 1703.
(44) Davis, C. T.; Ebel, G. D.; Lanciotti, R. S.; Brault, A. C.; Guzman, H.; Siirin, M.; Lambert, A.; Parsons, R. E.; Beasley, D. W.; Novak, R. J.; Elizondo-Quiroga, D.; Green, E. N.; Young, D. S.; Stark, L. M.; Drebot, M. A.; Artsob, H.; Tesh, R. B.; Kramer, L. D.; Barrett, A. D. Phylogenetic Analysis of North American West Nile Virus Isolates, 2001−2004: Evidence for the Emergence of a Dominant Genotype. *Virology* **2005**, *342*, 252.
(45) Payne, A. F.; Binduga-Gajewska, I.; Kauffman, E. B.; Kramer, L. D. Quantitation of Flaviviruses by Fluorescent Focus Assay. *J. Virol. Methods* **2006**, *134*, 183.
(46) Okon, A.; Han, J.; Dawadi, S.; Demosthenous, C.; Aldrich, C. C.; Gupta, M.; Wagner, C. R. Anchimerically Activated ProTides as Inhibitors of Cap-Dependent Translation and Inducers of Chemosensitization in Mantle Cell Lymphoma. *J. Med. Chem.* **2017**, *60*, 8131.
(47) Hexum, J. K.; Tello-Aburto, R.; Struntz, N. B.; Harned, A. M.; Harki, D. A. Bicyclic Cyclohexenones as Inhibitors of NF-κB Signaling. *ACS Med. Chem. Lett.* **2012**, *3*, 459.
(48) Gohara, D. W.; Ha, C. S.; Kumar, S.; Ghosh, B.; Arnold, J. J.; Wisniewski, T. J.; Cameron, C. E. Production of ″Authentic″ Poliovirus RNA-Dependent RNA Polymerase (3D^{Pol}) by Ubiquitin-Protease-Mediated Cleavage in *Escherichia Coli*. *Protein Expression Purif.* **1999**, *17*, 128.
(49) Huang, L.; Sineva, E. V.; Hargittai, M. R. S.; Sharma, S. D.; Suthar, M.; Raney, K. D.; Cameron, C. E. Purification and Characterization of Hepatitis C Virus Non-Structural Protein 5a Expressed in *Escherichia Coli*. *Protein Expression Purif.* **2004**, *37*, 144.